Cancer Science
The official journal of the Japanese Cancer Association

Miniaturized antibodies for imaging membrane type-1 matrix metalloproteinase in cancers

Naoya Kondo,[1] Takashi Temma,[1] Yoichi Shimizu,[1] Hiroyuki Watanabe,[1] Keiichi Higano,[2] Yoko Takagi,[2] Masahiro Ono[1] and Hideo Saji[1,3]

[1]Department of Patho-Functional Bioanalysis, Graduate School of Pharmaceutical Sciences, Kyoto University, Kyoto; [2]Biotechnology Research Department, Kyoto Electronics Manufacturing Company, Kyoto, Japan

(Received August 27, 2012/Revised December 25, 2012/Accepted December 26, 2012/Accepted manuscript online January 10, 2013/Article first published online February 17, 2013)

Since membrane type-1 matrix metalloproteinase (MT1-MMP) plays pivotal roles in tumor progression and metastasis and holds great promise as an early biomarker for malignant tumors, a method of evaluating MT1-MMP expression levels would be valuable for molecular biological and clinical studies. Although we have previously developed a ^{99m}Tc-labeled anti-MT1-MMP monoclonal IgG (^{99m}Tc-MT1-mAb) as an MT1-MMP imaging probe by nuclear medical techniques for this purpose, slow pharmacokinetics were a problem due to its large molecular size. Thus, in this study, our aim was to develop miniaturized antibodies, a single chain antibody fragment (MT1-scFv) and a dimer of two molecules of scFv (MT1-diabody), as the basic structures of MT1-MMP imaging probes followed by *in vitro* and *in vivo* evaluation with an ^{111}In radiolabel. Phage display screening successfully provided MT1-scFv and MT1-diabody, which had sufficiently high affinity for MT1-MMP (K_D = 29.8 and 17.1 nM). Both ^{111}In labeled miniaturized antibodies showed higher uptake in MT1-MMP expressing HT1080 cells than in non-expressing MCF7 cells. An *in vivo* biodistribution study showed rapid pharmacokinetics for both probes, which exhibited >20-fold higher tumor to blood radioactivity ratios (T/B ratio), an index for *in vivo* imaging, than ^{99m}Tc-MT1-mAb 6 h post-administration, and significantly higher tumor accumulation in HT1080 than MCF7 cells. SPECT images showed heterogeneous distribution and *ex vivo* autoradiographic analysis revealed that the radioactivity distribution profiles in tumors corresponded to MT1-MMP-positive areas. These findings suggest that the newly developed miniaturized antibodies are promising probes for detection of MT1-MMP in cancer cells. (*Cancer Sci* 2013; 104: 495–501)

Tumor metastasis is the most frequent cause of death for cancer patients. In order to metastasize, tumor cells must acquire the ability to break through the basement membrane and invade dense networks of interstitial ECM proteins.[1] Matrix metalloproteinases (MMPs) are a family of enzymes responsible for degrading the various ECM components. While most MMPs are secreted as soluble zymogens, members of the subfamily of membrane-type MMPs (MT-MMPs) anchored to the cell membrane are suited for pericellular proteolysis.[2,3] MT1-MMP is the major pericellular protease involved in processing triple helical collagen type I.[4] In addition, MT1-MMP activates MMP zymogens such as proMMP-2 and proMMP-13 that have significant involvement in tumor cell invasion and metastasis.[5,6] As MT1-MMP has a close relationship with tumor malignancy and holds great promise as an early biomarker of malignant tumors,[7,8] *in vivo* monitoring and/or quantitation of MT1-MMP expression could be valuable tools for molecular biological and clinical studies.

Recently, in the course of focusing on nuclear medical techniques for noninvasive quantitative evaluation of biological molecules deep within the body, we developed a ^{99m}Tc-labeled anti-MT1-MMP monoclonal IgG (^{99m}Tc-MT1-mAb) as a radiolabeled probe for nuclear medical imaging of MT1-MMP. Although this probe accumulated in the tumors of rodent models with a low effective dose,[9] blood clearance was slow and the tumor to blood (T/B) ratio, an indicator of radiotracer availability for *in vivo* imaging, remained low up to 48 h post-injection due to its high molecular weight (approximately 150 kDa), which led to a high systemic background radioactivity that prevented clear *in vivo* MT1-MMP imaging. Improvement of this imaging probe was necessary for further applications.

Thus, we planned to develop two miniaturized structural variants (scFv, diabody) of the anti-MT1-MMP antibody to improve the kinetics for cancer imaging.[10] scFv, single-chain Fv, is a 30 kDa molecule composed of a variable region of the light chain (V_L) and a variable region of the heavy chain (V_H) joined via a peptide spacer sequence. As a monovalent fragment, scFv was expected to show extremely rapid kinetics due to its small size. On the other hand, the diabody, a dimer of scFv, was expected to show high sensitivity as an *in vivo* imaging agent[11] due to its bivalency. Initially, scFv (MT1-scFv) and diabody (MT1-diabody) with affinity for MT1-MMP were identified using phage display technology. Next, ^{111}In-labeled MT1-scFv (^{111}In-MT1-scFv) and MT1-diabody (^{111}In-MT1-diabody) were prepared and evaluated for MT1-MMP imaging of cancers.

Materials and Methods

Preparation of MT1-scFv and MT1-diabody. We described the construction of phage display library in Data S1. The resulting library was subjected to five rounds of panning. After panning, ELISA assays were performed to select promising phages. Promising scFv (MT1-scFv) and diabody (MT1-diabody) were expressed (detail in Data S1) and purified by HisTALON Gravity Columns (Takara Bio, Tokyo, Japan), and then analyzed by 5–20% SDS-PAGE. We also prepared anti-polychlorobiphenyl scFv (NC-scFv) as a negative control.

Radiolabeling. MT1-scFv, MT1-diabody, and NC-scFv in 50 mM $NaHCO_3$ (pH 8.6) were mixed with 20 times equivalents of *p*-SCN-Bn-DTPA (10 mg/mL; Macrocyclics, Dallas, TX, USA) for 1 h at room temperature (rt). Unreacted *p*-SCN-Bn-DTPA was removed by size exclusion with an Amicon Ultra-4 Centrifugal Filter Unit (10k) (Millipore, Billerica, MA, USA) concomitant with solvent exchange in 0.1 M acetate buffer (pH 6.0). Next, $^{111}InCl_3$ (37 kBq/μg protein) was added and incubated for 1 h at rt. ^{111}In-labelled MT1-scFv, MT1-diabody, and NC-scFv (^{111}In-MT1-scFv, ^{111}In-MT1-diabody and ^{111}In-NC-scFv) were purified into molecular weight (MW)-

[3]To whom correspondence should be addressed.
E-mail: hsaji@pharm.kyoto-u.ac.jp

doi: 10.1111/cas.12102

dependent fractions (250 μL × 60 fractions) by size exclusion chromatography on Superdex 75 10/300 GL (GE Healthcare, Tokyo, Japan) eluting with PBS(−) followed by radioactivity counting with a NaI well-type scintillation counter (1470 WIZARD; PerkinElmer, Yokohama, Japan).

Immunoreactivity analysis. Surface plasmon resonance was analyzed with the ProteOn XPR36 system (Bio-rad Laboratories, Tokyo, Japan). MT1-MMP protein (ag6062; Proteintech Group, Chicago, IL, USA) or hinge region peptide conjugated with BSA (described in detail in Data S1) was coupled onto a GLM chip. MT1-scFv, MT1-diabody (unconjugated or DTPA-conjugated) and NC-scFv solutions, prepared as threefold serial dilutions (0, 7.7–625 nM), were injected onto the chip. The resulting sensorgrams were fitted by the simplest 1:1 interaction model using ProteOn analysis software to obtain the corresponding association and dissociation rate constants. Other determinations (antigen-immobilized ELISA, cell ELISA, and indirect competitive ELISA) are described in Data S1.

Cellular uptake study. HT1080 human fibrosarcoma cells and MCF7 human breast adenocarcinoma cells, supplied by ATCC, were cultured in DMEM (Nissui Pharmaceutical, Tokyo, Japan) with 10% FBS at 37°C in a humidified atmosphere containing 5% CO_2. HT1080 or MCF7 (5×10^5 cells) in FBS-free-DMEM were added to eppendorf tubes and were incubated with ^{111}In-MT1-scFv, ^{111}In-MT1-diabody or ^{111}In-NC-scFv. After 1 or 3 h, cells were washed with PBS(−), lysed with 0.2 M NaOH, and then counted for radioactivity. Protein quantitation was performed by the BCA protein assay (Thermo Fisher Scientific, Yokohama, Japan).

Preparation of tumor-bearing mice. Female Balb/c nu-nu mice (5 weeks old; Japan SLC, Hamamatsu, Japan) and female SCID mice (5 weeks old; CLEA, Tokyo, Japan) were housed under a 12/12 h light/dark cycle and were given free access to food and water. Animal experiments were conducted in accordance with institutional guidelines and were approved by the Kyoto University Animal Care Committee. HT1080 cells were suspended in PBS(−) followed by subcutaneous inoculation into the right hind legs of Balb/c and SCID mice (5×10^6 cells/100 μL) and MCF7 cells (2×10^7 cells/100 μL) were injected into the left hind legs.

***In vivo* study.** Animals were divided into groups (n = 3–4) for time points with approximately equal distribution of tumor sizes on the day before the study. Animals were fasted for 6 h before administration of the radiopharmaceutical. At time points 15 min, 1, 3, 6, and 24 h after intravenous administration of ^{111}In-MT1-scFv or ^{111}In-MT1-diabody (18.5 kBq/100 μL saline), mice were killed. The blood, heart, lung, liver, kidney, stomach, intestine, spleen, pancreas, muscle, and tumor tissues were excised, weighed, and counted for radioactivity. HT1080 and MCF7 cells co-implantation model SCID mice were killed at 1 or 24 h for ^{111}In-MT1-scFv and 3 or 24 h for ^{111}In-MT1-diabody (18.5 kBq/100 μL saline), and tumor tissues were excised.

***Ex vivo* autoradiography and immunohistochemistry.** Tumor-bearing mice were killed 3 h after intravenous administration of ^{111}In-MT1-scFv or ^{111}In-NC-scFv and 24 h of the ^{111}In-MT1-diabody (740 kBq/mouse). The tumors were removed and immediately frozen. After freezing, 10-μm thick sections of the tumor were prepared with a cryomicrotome (CM1900; Leica Microsystems, Tokyo, Japan) and exposed to imaging plates (BAS-SR; Fuji Photo Film, Tokyo, Japan) for 10 days. Autoradiograms of these sections were obtained with a BAS5000 scanner (Fuji Photo Film). Adjacent sections of the autoradiographic study were subjected to immunostaining against MT1-MMP (described in details in Data S1).

SPECT/CT imaging study. ^{111}In-MT1-scFv and ^{111}In-MT1-diabody (13.0 MBq) were injected into HT1080 tumor-bearing mice. The mice were anesthetized by isoflurane and SPECT and CT images were obtained using the U-SPECT-II system (MILabs, Utrecht, the Netherlands) with 1.0-mm pinhole collimators (SPECT conditions; 30 min × 1 frame, CT conditions; accurate full angle mode in 65 kV/615 μA) 3 h after injection of the ^{111}In-MT1-scFv or ^{111}In-MT1-diabody. SPECT images were reconstructed by the OSEM method (one subset, 40 iterations) with a 1.6-mm Gaussian filter with ^{111}In-MT1-scFv and a 0.9 mm filter for ^{111}In-MT1-diabody.

Statistics. Data are presented as means ± SD. The Mann–Whitney U-test was used to evaluate the significance of differences in the cellular uptake and *in vivo* studies. Differences at the 95% confidence level ($P < 0.05$) were considered significant.

Results

***In vitro* characterization.** Sodium dodecyl sulfate-PAGE analysis showed the MT1-scFv and MT1-diabody as single bands (Fig. 1a). Enzyme linked immunosorbent assay revealed that both modified antibodies (MT1-scFv and MT1-diabody) had affinity and specificity for the antigen (MT1-MMP hinge region) peptide as well as affinity for MT1-MMP expressing cancer cells (Table S1). ProteOn revealed K_D dissociation constants for MT1-scFv and MT1-diabody of 29.8 ± 4.1 and 17.1 ± 4.0 nM, respectively, against immobilized MT1-MMP protein. MT1-scFv and MT1-diabody also showed high affinity for the hinge region peptide of MT1-MMP (TKMPPQPRTTSRPS VPDKPKN) (K_D = 51.1 ± 30.3, 0.27 ± 0.21 nM, respectively), but did not bind to a scrambled peptide (RKPRQPTSPTKPM VSNPTPDK). After conjugation with the bifunctional chelating agent (*p*-SCN-Bn-DTPA), the K_D of MT1-scFv and MT1-diabody were determined to be 38.5 ± 1.3 and 26.5 ± 2.9 nM, respectively. NC-scFv did not show affinity for MT1-MMP.

Radiolabeling. The MT1-scFv, MT1-diabody and NC-scFv were efficiently labeled with ^{111}In in radiochemical yields and radiochemical purities evaluated as >95%. From size-exclusion chromatography analysis using a Superdex 75 10/300 GL, retention volumes (mL) of the major peaks of ^{111}In-MT1-scFv and ^{111}In-NC-scFv (11.0 mL) were almost exactly corresponded to 32 kDa myokinase (10.98 mL) (Fig. 1b,c,e). ^{111}In-MT1-diabody (9.25 mL) almost exactly corresponded to 67 kDa enolase (9.15 mL) (Fig. 1b,d).

Cellular uptake study. MT1-MMP expressing HT1080 and MT1-MMP non-expressing MCF7 cells were incubated with ^{111}In-MT1-scFv, ^{111}In-MT1-diabody and ^{111}In-NC-scFv followed by radioactivity measurement of the cells (Fig. 2). Radioactivities of HT1080 cells treated with ^{111}In-MT1-scFv and ^{111}In-MT1-diabody were significantly higher than those of MCF7 cells. HT1080 cells treated with ^{111}In-NC-scFv showed lower radioactivity, not significantly different from MCF7 cells.

***In vivo* study.** Biodistributions of ^{111}In-MT1-scFv and ^{111}In-MT1-diabody in tumor-bearing mice are shown in Tables 1 and 2, respectively. Both probes showed rapid blood clearance with 0.75 ± 0.14 and 0.10 ± 0.01%ID/g at 1 and 24 h after injection of ^{111}In-MT1-scFv, and 3.26 ± 0.37 and 0.09 ± 0.03%ID/g at 1 and 24 h after injection of ^{111}In-MT1-diabody. Radioactivities for T/B ratios of ^{111}In-MT1-scFv and ^{111}In-MT1-diabody are shown in Figure 3. The T/B ratio 1 h post-administration of ^{111}In-MT1-scFv was 2.23 ± 0.38, which was greater than fivefold higher than ^{111}In-MT1-diabody. The T/B ratio of the ^{111}In-MT1-diabody increased up to 6 h post-administration before reaching a plateau (6.15 ± 1.92 at 6 h, 5.86 ± 3.88 at 24 h). Tumor accumulation of both probes with HT1080 and MCF7 tumor cells in co-implantation model SCID mice are shown in Figure 4. ^{111}In-MT1-scFv gave a significantly higher accumulation with HT1080 (2.60 ± 0.19 at 1 h, 2.78 ± 0.24 at 24 h) than MCF7 cells (2.20 ± 0.15 at

doi: 10.1111/cas.12102

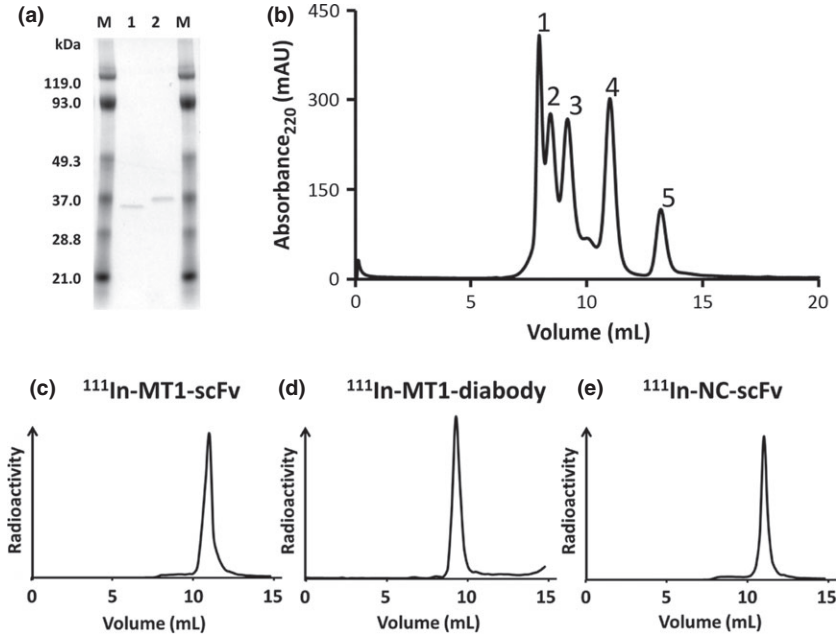

Fig. 1. (a) Sodium dodecyl sulfate-polyacrylamide gel electrophoresis (SDS-PAGE) of MT1-scFv (1) and MT1-diabody (2). (b) Chromatograms of MW-marker; 1 (7.93 mL), glutamate dehydrogenase 290 kDa: 2 (8.43 mL), lactate dehydrogenase 142 kDa: 3 (9.15 mL), enolase 67 kDa: 4 (10.98 mL), myokinase 32 kDa: 5 (13.18 mL), cytochrome C 12.4 kDa. (c) Chromatogram of ^{111}In-MT1-scFv (11.0 mL). (d) Chromatogram of ^{111}In-MT1-diabody (9.25 mL). (e) Chromatogram of ^{111}In-NC-scFv (11.0 mL).

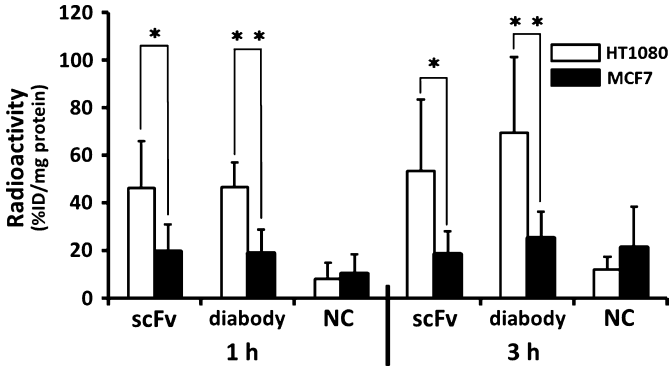

Fig. 2. The radioactivity of HT1080 cells and MCF-7 cells after incubation for 1 and 3 h with ^{111}In-MT1-scFv (scFv), ^{111}In-MT1-diabody (diabody) and ^{111}In-NC-scFv (NC). Data are expressed as radioactivity per cell protein (mg) (mean ± standard deviation [SD]). Comparison between HT1080 and MCF-7 cell groups was performed with the Mann–Whitney *U*-test (**P* < 0.005, ***P* < 0.0001 versus MCF-7).

1 h, 2.19 ± 0.43 at 24 h). The ^{111}In-MT1-diabody had also significantly higher accumulation with HT1080 (2.25 ± 0.39 at 3 h, 2.06 ± 0.12 at 24 h) than MCF7 cells (1.80 ± 0.12 at 3 h, 1.79 ± 0.15 at 24 h).

SPECT/CT imaging study. SPECT images obtained 3 h after administration of the ^{111}In-MT1-scFv and ^{111}In-MT1-diabody showed heterogeneous distribution of radioactivity. Transverse, sagittal and coronal images are shown in Figure 5.

***Ex vivo* autoradiography and immunohistochemistry.** Autoradiograms showed that the distributions of ^{111}In-MT1-scFv, ^{111}In-MT1-diabody and ^{111}In-NC-scFv in tumors were heterogeneous (Fig. 6b,d,f). Immunohistochemistry indicated the presence of MT1-MMP areas in tumors (Fig. 6a,c,e). The accumulation profiles of ^{111}In-MT1-scFv and ^{111}In-MT1-diabody tended to correspond to MT1-MMP positive areas, but ^{111}In-NC-scFv didn't.

Discussion

The results of affinity analysis indicated that both probes had sufficiently high affinity for MT1-MMP imaging and that both

Table 1. Biodistribution of radioactivity after injection of ^{111}In-MT1-scFv in tumor-bearing mice†

	Time after injection (h)				
	0.25	1	3	6	24
Blood	3.36 ± 0.53	0.75 ± 0.14	0.38 ± 0.07	0.26 ± 0.03	0.10 ± 0.01
Heart	0.82 ± 0.36	1.33 ± 0.27	0.71 ± 0.19	0.70 ± 0.07	0.49 ± 0.08
Lung	6.36 ± 1.58	1.72 ± 0.32	0.80 ± 0.26	0.62 ± 0.26	0.41 ± 0.17
Liver	25.87 ± 3.03	23.41 ± 2.38	21.24 ± 7.83	23.29 ± 0.91	14.80 ± 1.38
Kidney	249.93 ± 15.08	237.53 ± 23.96	220.34 ± 48.95	225.90 ± 8.71	182.00 ± 8.53
Stomach‡	0.34 ± 0.07	0.20 ± 0.03	0.14 ± 0.02	0.19 ± 0.00	0.14 ± 0.04
Intestine	1.51 ± 0.11	0.85 ± 0.26	1.59 ± 0.62	1.48 ± 0.22	0.73 ± 0.11
Pancreas	1.66 ± 0.45	1.19 ± 0.22	0.85 ± 0.19	0.90 ± 0.03	0.64 ± 0.17
Spleen	16.90 ± 2.66	7.87 ± 1.71	6.00 ± 2.76	6.14 ± 1.16	5.77 ± 0.37
Muscle	0.96 ± 0.59	0.71 ± 0.04	0.65 ± 0.12	0.58 ± 0.19	0.45 ± 0.08
Tumor	0.71 ± 0.50	1.68 ± 0.51	1.35 ± 0.20	1.14 ± 0.22	0.64 ± 0.17

†Tissue radioactivity is expressed as % injected dose per gram. ‡Expressed as % injected dose.

Table 2. Biodistribution of radioactivity after injection of ^{111}In-MT1-diabody in tumor bearing mice†

	Time after injection (h)				
	0.25	1	3	6	24
Blood	7.30 ± 1.18	3.26 ± 0.37	1.64 ± 0.12	0.21 ± 0.04	0.09 ± 0.03
Heart	1.78 ± 0.42	1.80 ± 0.32	1.34 ± 0.15	0.82 ± 0.06	0.59 ± 0.13
Lung	4.34 ± 0.55	2.04 ± 0.34	1.51 ± 0.24	0.40 ± 0.2	0.61 ± 0.10
Liver	47.00 ± 4.61	39.68 ± 3.56	40.63 ± 3.13	26.75 ± 1.64	15.96 ± 3.03
Kidney	65.98 ± 11.65	108.2 ± 15.05	131.98 ± 8.44	97.98 ± 10.66	241.74 ± 28.36
Stomach‡	0.71 ± 0.06	1.27 ± 0.32	0.98 ± 0.33	1.29 ± 1.03	0.49 ± 0.22
Intestine	0.56 ± 0.12	1.14 ± 0.17	2.21 ± 0.13	2.14 ± 0.91	0.85 ± 0.17
Pancreas	0.52 ± 0.08	0.47 ± 0.07	0.56 ± 0.12	0.57 ± 0.07	0.83 ± 0.06
Spleen	13.03 ± 2.43	8.77 ± 1.47	8.34 ± 0.65	6.31 ± 0.36	6.50 ± 1.33
Muscle	0.29 ± 0.12	0.35 ± 0.08	0.29 ± 0.09	0.47 ± 0.53	0.94 ± 0.58
Tumor	1.14 ± 0.18	1.35 ± 0.33	1.52 ± 0.13	1.37 ± 0.73	0.47 ± 0.24

†Tissue radioactivity is expressed as % injected dose per gram. ‡Expressed as % injected dose.

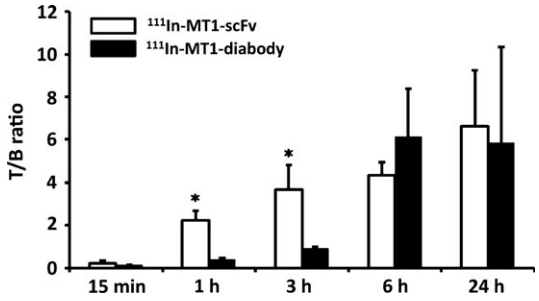

Fig. 3. Tumor to blood radioactivity ratio (T/B) of ^{111}In-MT1-scFv and ^{111}In-MT1-diabody. Comparisons between ^{111}In-MT1-scFv and ^{111}In-MT1-diabody were performed with the Mann–Whitney *U*-test (*P < 0.05 versus ^{111}In-MT1-diabody).

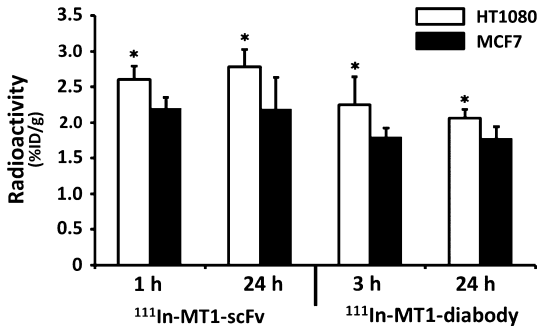

Fig. 4. Tumor accumulations of ^{111}In-MT1-scFv (1, 24 h) and ^{111}In-MT1-diabody (3, 24 h) in HT1080 and MCF7 tumors. Comparisons of accumulations between HT1080 and MCF7 were performed with the Mann–Whitney *U*-test (*P < 0.05 versus MCF7).

were successfully radiolabeled with ^{111}In. Biodistribution studies in tumor-bearing mice demonstrated that ^{111}In-MT1-scFv and ^{111}In-MT1-diabody had rapid blood clearance. The T/B ratio, an important index for *in vivo* imaging, of the ^{111}In-MT1-scFv and ^{111}In-MT1-diabody was about 20-fold higher than the previously reported whole body antibody probe (^{99m}Tc-MT1-mAb[9]) 6 h post-administration, suggesting that the newly developed ^{111}In labeled miniaturized antibodies have potential for clinical evaluation. In addition, the rapid pharmacokinetics of these agents may allow adoption of ^{99m}Tc, the most useful generator-produced radioisotope with a short (6 h) half-life, as the signal moiety instead of ^{111}In.

MT1-MMP comprises several domains that include propeptide, catalytic, hinge region, hemopexin, and transmembrane domains and a cytoplasmic tail.[12] Recently, several research groups have revealed non-proteolytic roles for MT1-MMP in tumor malignancy.[13,14] Therefore, in this study, we proposed to evaluate not proteolytic activity, but the expression level of MT1-MMP, in which case the extracellular domains of MT1-MMP could be targeted. However, the propeptide and the catalytic domain are eliminated from the cell membrane by an autocatalytic processing.[15,16] The hemopexin domain is involved in various interactions.[17,18] Therefore, other proteins may interfere with binding to the hemopexin domain. Thus, we decided to target the hinge region of MT1-MMP. Promising clones (including MT1-scFv and MT1-diabody) were first obtained using phage-display technology. Next, expressed and purified clones were evaluated for their affinity to immobilized antigen by ELISA. Enzyme linked immunosorbent assay revealed the MT1-scFv and MT1-diabody had higher affinity for MT1-MMP hinge region than other clones. ProteOn analysis revealed the MT1-diabody had better affinity than MT1-scFv, which may result from its bivalency. Furthermore, ProteOn revealed both probes specifically recognized the hinge region sequence, which does not share homology with other MMPs. Thus, MT1-scFv and MT1-diabody are believed to be free from cross-reactivity with other MMPs. Radiolabeling with ^{111}In was successfully performed with high radiochemical yield and radiochemical purity (>95%), which meant the conjugates could be used for *in vitro* and *in vivo* experiments without additional purification. Furthermore, ProteOn revealed the affinity of both probes for MT1-MMP was not affected by conjugation with *p*-SCN-Bn-DTPA.

To evaluate immunoreactivity for MT1-MMP on cancer cells, a cellular uptake study was performed using HT1080 as MT1-MMP positive cells and MCF7 cells as MT1-MMP negative cells in a Western blot analysis.[19] We used ^{111}In-MT1-scFv and ^{111}In-MT1-diabody, in addition, ^{111}In-NC-scFv was used to evaluate nonspecific uptake into tumor cells. Although ^{111}In-NC-scFv showed low accumulation in both HT1080 and MCF7 cells, the ^{111}In-MT1-scFv and ^{111}In-MT1-diabody showed significantly high accumulation in HT1080 indicating both had affinity for MT1-MMP in cells and retained their immunoreactivity for MT1-MMP after conjugation with *p*-SCN-Bn-DTPA and radiolabeling with ^{111}In.

Biodistribution studies of ^{111}In-MT1-scFv and ^{111}In-MT1-diabody in tumor-bearing mice indicated their rapid blood clearance, especially in the 1–3 h period after injection, with faster blood clearance of ^{111}In-MT1-scFv than the ^{111}In-diabody because of its smaller size. High radioactivity in the kidneys indicated renal excretion of the probes. The T/B ratio 1 h after injection of ^{111}In-MT1-scFv was more than 5- and 30-fold higher than the ^{111}In-MT1-diabody and our previously reported ^{99m}Tc-MT1-mAb, respectively, indicating that the

doi: 10.1111/cas.12102

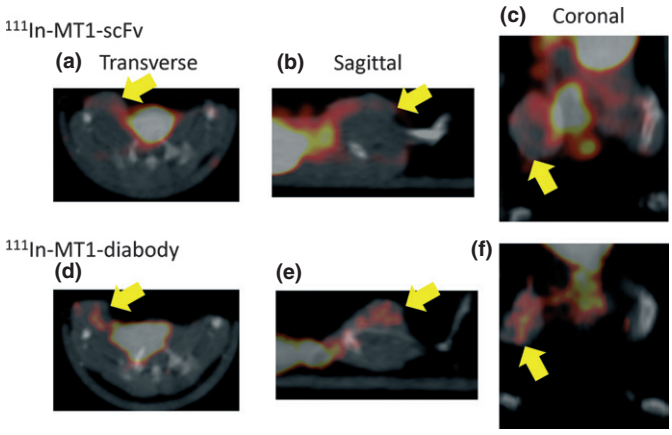

Fig. 5. Transverse, sagittal and coronal images of tumor-bearing mice 3 h after administration with ^{111}In-MT1-scFv (a–c) and ^{111}In-MT1-diabody (d–f). Yellow arrows indicate tumors.

scFv format would be useful for imaging cancers shortly after being injected. The T/B ratios of ^{111}In-MT1-scFv and ^{111}In-MT1-diabody after 6 h were similar; however, tumor accumulation of ^{111}In-MT1-diabody was higher than ^{111}In-MT1-scFv and had lower accumulation in the kidneys, suggesting ^{111}In-MT1-diabody would be more suitable for high sensitivity cancer imaging and/or a lower injection dose than ^{111}In-MT1-scFv. Thus, both agents could shorten the time for cancer imaging compared to the previous mAb imaging agent.

The SPECT/CT imaging study indicated both probes showed heterogeneous distribution in tumors. We found that the ^{111}In-MT1-diabody gave clearer tumor imaging than the ^{111}In-MT1-scFv due to higher accumulation in tumors. In the coronal image of ^{111}In-MT1-scFv, we found relatively high radioactivity, which was not derived from tissues around the tumor. We believe this radioactivity was caused by excreted urine.

Furthermore, we confirmed probe accumulation into HT1080 and MCF7 tumor cells in co-implantation model SCID mice. Both ^{111}In-MT1-scFv and ^{111}In-MT1-diabody showed significantly higher accumulation into HT1080 cells. Finally, *ex vivo* autoradiography and immunohistochemistry were examined to confirm the accumulation of ^{111}In-MT1-scFv and ^{111}In-MT1-diabody in HT1080 tumors according to MT1-MMP expression. Consequently, these radioactivity distribution profiles corresponded to MT1-MMP-positive areas. These data indicate both probes maintained an affinity for MT1-MMP *in vivo*, and the accumulation in tumors did reflect MT1-MMP expression.

Many research groups have been developing *in vivo* imaging probes for MT1-MMP. In fact, some fluorogenic probes activated by or binding with MT1-MMP have successfully imaged tumors.[20–22] However, these probes were insufficient for quantitative analysis of MT1-MMP *in vivo*. In this regard, radiolabeled probes were expected to achieve more accurate quantitation; therefore, several radiolabeled probes for MT1-MMP have been developed including the ^{99m}Tc-MT1-mAb[9] and ^{123}I-labelled TIMP-2.[23] However, ^{99m}Tc-MT1-mAb displayed a relatively low T/B ratio because of the large molecular size of the mAb, and tumor accumulation of ^{123}I-labelled TIMP-2 was inhibited by endogenous TIMP-2. Furthermore, TIMP-2 also had affinity for MMP-2. This broad-spectrum among MMPs is problematic in terms of MT1-MMP quantitation. To improve the T/B ratio, we previously reported using a pre-targeting method.[24] While this modification improved the T/B ratio, the method required multiple administrations, which would be undesirable for clinical use. In this study, the newly developed ^{111}In-MT1-scFv and ^{111}In-MT1-diabody showed specific affinity for MT1-MMP hinge region and gave high T/B ratios. The specificity of these agents for MT1-MMP and their good contrast would improve quantitation of MT1-MMP expression levels and could contribute to molecular biological and clinical studies. MT1-MMP is thought to be a promising predictor for recurrence risk in early stage breast cancer.[25] Although accumulation of ^{111}In-MT1-scFv and ^{111}In-MT1-diabody in abdominal tissues like kidney, liver, spleen and intestine for excretion would hamper imaging tumors, we expect both probes to be used for breast cancer imaging, which is less affected by the background radioactivity of surrounding tissues because breast cancers are typically located from these other tissues.

For further applications involving imaging of other cancers, non-specific accumulation in other tissues should be decreased. For instance, imaging for pancreatic cancers would be hampered by non-specific accumulation in the liver. One of the possible reasons for non-specific accumulation may be the cationic character of both probes (pI of MT1-scFv: 9.54, MT1-diabody: 9.40). Because cationic probes typically have increased tissue retention, non-specific accumulation may be reduced by anionization, such as converting positively charged groups into negatively charged groups, while maintaining the immunoreactivity of the probes.[26] High accumulation in the kidneys could be overcome by radiolabeling with a renal enzyme-cleavable linkage.[27]

Increasing the accumulation in tumors is a straightforward strategy for clearly imaging cancers. To increase the accumulation of the probes in tumors, we believe affinity for MT1-MMP is an important factor. Since the diabody can bind to

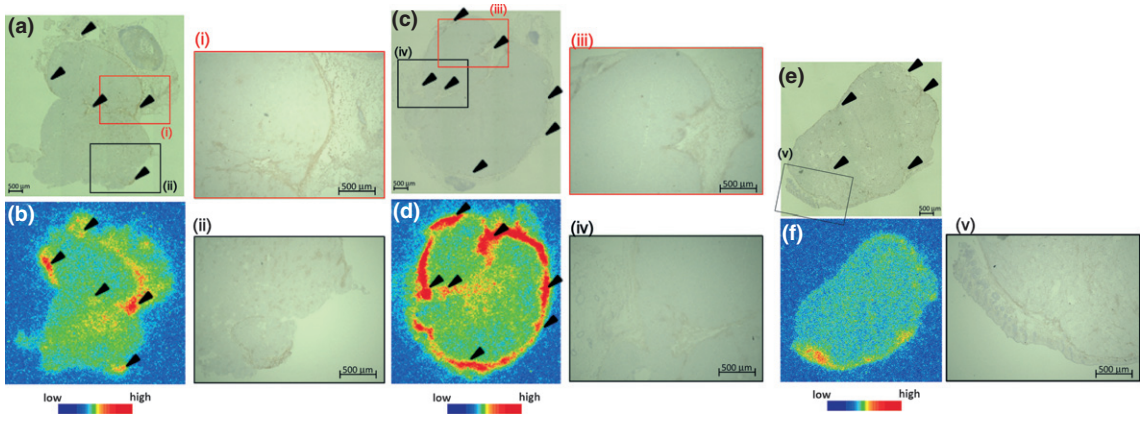

Fig. 6. Representative images of MT1-MMP immunostainings and autoradiograms of ^{111}In-MT1-scFv (a,b), ^{111}In-MT1-diabody (c,d), and ^{111}In-NC-scFv (e,f). Black arrowheads indicate areas of MT1-MMP expression.

antigen in a bivalent manner, we expected the MT1-diabody to have a higher affinity for MT1-MMP than MT1-scFv. Consequently, the MT1-diabody showed an extremely high affinity against the hinge region peptide (K_D = 0.27 nM), but it showed mediocre affinity for MT1-MMP protein. We postulated that the recognition site of MT1-diabody might be blocked to some degree by the secondary structure of MT1-MMP. We believe converting MT1-scFv into the diabody form by shortening the linker would be an effective alternative method. The converted MT1-scFv could acquire higher affinity through bivalent binding.[28] We consider higher specific radioactivity could also be effective. In this study, we administered ^{111}In-MT1-scFv and ^{111}In-MT1-diabody (18.5 kBq/0.5 μg protein) to mice. Although these conditions were similar to previously reported conditions from other researchers,[29,30] about 1000-fold unlabeled MT1-scFv and MT1-diabody used as precursors were also administered with ^{111}In-MT1-scFv and ^{111}In-MT1-diabody and might block binding sites on MT1-MMP to some extent. Therefore, decreasing the amount of unlabeled precursor, which could be achieved by refining the reaction conditions, may lead to increased specific accumulation in tumors. These attempts would lead to increased specific accumulation and allow a more precise evaluation of MT1-MMP expression in tumors.

As this research constitutes a preliminary study of miniaturized antibodies for imaging MT1-MMP, there are a number of further modifications that could improve the characteristics of these imaging agents.

In conclusion, we have developed novel ^{111}In labeled MT1-MMP imaging probes based on scFv and diabody (MT1-scFv and MT1-diabody) for sensitive cancer imaging within a short time after administration. Compared with the previously developed whole antibody probe, faster blood clearance and sufficiently higher T/B ratios during the early period after administration with the new agents were achieved. This study shows the strategy of using antibody fragments is effective for improving the kinetics of imaging MT1-MMP in cancer cells, and both novel probes have the potential for further applications.

Acknowledgments

This study was partly supported by Grants-in-Aid for Scientific Research (22791189 and 23113509) from the Ministry of Education, Culture, Sports, Science and Technology, Japan. Part of this study was supported by the New Energy and Industrial Technology Development Organization (NEDO), Japan.

Disclosure Statement

The authors have no conflict of interest.

References

1 Yamaguchi H, Wyckoff J, Condeelis J. Cell migration in tumors. *Curr Opin Cell Biol* 2005; **17**: 559–64.
2 Page-McCaw A, Ewald AJ, Werb Z. Matrix metalloproteinases and the regulation of tissue remodelling. *Nat Rev Mol Cell Biol* 2007; **8**: 221–33.
3 Jones JL, Glynn P, Walker RA. Expression of MMP-2 and MMP-9, their inhibitors, and the activator MT1-MMP in primary breast carcinomas. *J Pathol* 1999; **189**: 161–8.
4 Ohuchi E, Imai K, Fujii Y, Sato H, Seiki M, Okada Y. Membrane type 1 matrix metalloproteinase digests interstitial collagens and other extracellular matrix macromolecules. *J Biol Chem* 1997; **272**: 2446–51.
5 Knäuper V, Will H, López-Otin C *et al.* Cellular mechanisms for human procollagenase-3 (MMP-13) activation. Evidence that MT1-MMP (MMP-14) and gelatinase a (MMP-2) are able to generate active enzyme. *J Biol Chem* 1996; **271**: 17124–31.
6 Itoh Y, Seiki M. MT1-MMP: a potent modifier of pericellular microenvironment. *J Cell Physiol* 2006; **206**: 1–8.
7 Brinckerhoff CE, Matrisian LM. Matrix metalloproteinases: a tail of a frog that became a prince. *Nat Rev Mol Cell Biol* 2002; **3**: 207–14.
8 Crispi S, Calogero RA, Santini M *et al.* Global gene expression profiling of human pleural mesotheliomas: identification of matrix metalloproteinase 14 (MMP-14) as potential tumour target. *PLoS ONE* 2009; **4**: e7016.
9 Temma T, Sano K, Kuge Y *et al.* Development of a radiolabeled probe for detecting membrane type-1 matrix metalloproteinase on malignant tumors. *Biol Pharm Bull* 2009; **32**: 1272–7.
10 Holliger P, Hudson PJ. Engineered antibody fragments and the rise of single domains. *Nat Biotechnol* 2005; **23**: 1126–36.
11 Sundaresan G, Yazaki PJ, Shively JE *et al.* 124I-labeled engineered anti-CEA minibodies and diabodies allow high-contrast, antigen-specific small-animal PET imaging of xenografts in athymic mice. *J Nucl Med* 2003; **44**: 1962–9.
12 Nagase H, Woessner JF Jr. Matrix metalloproteinases. *J Biol Chem* 1999; **274**: 21491–4.
13 D'Alessio S, Ferrari G, Cinnante K *et al.* Tissue inhibitor of metalloproteinases-2 binding to membrane-type 1 matrix metalloproteinase induces MAPK activation and cell growth by a non-proteolytic mechanism. *J Biol Chem* 2008; **283**: 87–99.
14 Remacle AG, Golubkov VS, Shiryaev SA *et al.* Novel MT1-MMP small-molecule inhibitors based on insights into hemopexin domain function in tumor growth. *Cancer Res* 2012; **72**: 2339–49.
15 Yana I, Weiss SJ. Regulation of membrane type-1 matrix metalloproteinase activation by proprotein convertases. *Mol Biol Cell* 2000; **11**: 2387–401.
16 Toth M, Hernandez-Barrantes S, Osenkowski P *et al.* Complex pattern of membrane type 1 matrix metalloproteinase shedding. Regulation by autocatalytic cells surface inactivation of active enzyme. *J Biol Chem* 2002; **277**: 26340–50.
17 Itoh Y, Ito N, Nagase H, Evans RD, Bird SA, Seiki M. Cell surface collagenolysis requires homodimerization of the membrane-bound collagenase MT1-MMP. *Mol Biol Cell* 2006; **17**: 5390–9.
18 Mori H, Tomari T, Koshikawa N *et al.* CD44 directs membrane-type 1 matrix metalloproteinase to lamellipodia by associating with its hemopexin-like domain. *EMBO J* 2002; **21**: 3949–59.
19 Atkinson JM, Falconer RA, Edwards DR *et al.* Development of a novel tumor-targeted vascular disrupting agent activated by membrane-type matrix metalloproteinases. *Cancer Res* 2010; **70**: 6902–12.
20 Shimizu Y, Temma T, Sano K, Ono M, Saji H. Development of membrane type-1 matrix metalloproteinase-specific activatable fluorescent probe for malignant tumor detection. *Cancer Sci* 2011; **102**: 1897–903.
21 Zhu L, Wang H, Wang L *et al.* High-affinity peptide against MT1-MMP for *in vivo* tumor imaging. *J Control Release* 2011; **150**: 248–55.
22 Zhu L, Zhang F, Ma Y *et al. In vivo* optical imaging of membrane-type matrix metalloproteinase (MT-MMP) activity. *Mol Pharm* 2011; **8**: 2331–8.
23 Van Steenkiste M, Oltenfreiter R, Frankenne F *et al.* Membrane type 1 matrix metalloproteinase detection in tumors, using the iodinated endogenous [123I]-tissue inhibitor 2 of metalloproteinases as imaging agent. *Cancer Biother Radiopharm* 2010; **25**: 511–20.
24 Sano K, Temma T, Kuge Y *et al.* Radioimmunodetection of membrane type-1 matrix metalloproteinase relevant to tumor malignancy with a pre-targeting method. *Biol Pharm Bull* 2010; **33**: 1589–95.
25 Ogura S, Ohdaira T, Hozumi Y, Omoto Y, Nagai H. Metastasis-related factors expressed in pT1 pN0 breast cancer: assessment of recurrence risk. *J Surg Oncol* 2007; **96**: 46–53.
26 Boswell CA, Tesar DB, Mukhyala K, Theil FP, Fielder PJ, Khawli LA. Effects of charge on antibody tissue distribution and pharmacokinetics. *Bioconjug Chem* 2010; **21**: 2153–63.
27 Uehara T, Koike M, Nakata H *et al.* Design, synthesis, and evaluation of [188Re]organorhenium-labeled antibody fragments with renal enzyme-cleavable linkage for low renal radioactivity levels. *Bioconjug Chem* 2007; **18**: 190–8.
28 Adams GP, Schier R, McCall AM *et al.* Prolonged *in vivo* tumour retention of a human diabody targeting the extracellular domain of human HER2/neu. *Br J Cancer* 1998; **77**: 1405–12.
29 Li L, Yazaki PJ, Anderson AL *et al.* Improved biodistribution and radioimmunoimaging with poly(ethylene glycol)-DOTA-conjugated anti-CEA diabody. *Bioconjug Chem* 2006; **17**: 68–76.
30 Lub-de Hooge MN, Kosterink JG, Perik PJ *et al.* Preclinical characterization of 111In-DTPA-Trastuzumab. *Br J Pharmacol* 2004; **143**: 99–106.

doi: 10.1111/cas.12102

Supporting Information

Additional Supporting Information may be found in the online version of this article:

Table S1. Data from the antigen-immobilized ELISA, indirect competitive ELISA, cell ELISA.

Data S1. Materials and Methods.